Journal of Cell Science 112, 4163-4171 (1999)
Printed in Great Britain © The Company of Biologists Limited 1999
JCS0811

Regulation of fibrillin carboxy-terminal furin processing by N-glycosylation, and association of amino- and carboxy-terminal sequences

Jane L. Ashworth[1], Vicky Kelly[1], Matthew J. Rock[1], C. Adrian Shuttleworth[1] and Cay M. Kielty[2,*]

Wellcome Trust Centre for Cell-Matrix Research, [1]School of Biological Sciences and [2]Department of Medicine, 2.205 Stopford Building, University of Manchester M13 9PT, UK
*Author for correspondence (e-mail: cay.kielty@man.ac.uk)

Accepted 16 September; published on WWW 3 November 1999

SUMMARY

The molecular mechanisms of fibrillin assembly into microfibrils are poorly understood. In this study, we investigated human fibrillin-1 carboxy-terminal processing and assembly using a recombinant approach. Processing of carboxy-terminal fibrillin-1 was strongly influenced by N-glycosylation at the site immediately downstream of the furin site, and by association with calreticulin. The carboxy terminus of fibrillin-2 underwent less efficient processing than carboxy-terminal fibrillin-1 under identical conditions. Size fractionation of the amino-terminal region of fibrillin-1, and of unprocessed and furin-processed carboxy-terminal region of fibrillin-1, revealed that the amino terminus formed abundant disulphide-bonded aggregates. Some association of unprocessed carboxy-terminal fibrillin-1 was also apparent, but processed carboxy-terminal sequences remained monomeric unless amino-terminal sequences encoded by exons 12-15 were present. These data indicate the presence of fibrillin-1 molecular recognition sequences within the amino terminus and the extreme carboxy-terminal sequence downstream of the furin site, and a specific amino- and carboxy-terminal association which could drive overlapping linear accretion of furin-processed fibrillin molecules in the extracellular space. Differences in processing of the two fibrillin isoforms may reflect differential abilities to assemble in the extracellular space.

Key words: Fibrillin, Furin, Processing, Calreticulin, Assembly

INTRODUCTION

Fibrillins are large cysteine-rich glycoproteins (~350 kDa) which form the molecular scaffold of a class of beaded microfibrils that are key structural elements of dynamic connective tissues (Kielty and Shuttleworth, 1995). These microfibrils are extensible polymers which act as a structural lattice for elastin deposition during elastic fibre formation (Mecham and Heusar, 1991). Linkage of the fibrillin-1 and fibrillin-2 genes to the heritable connective tissue disorders Marfan syndrome and congenital contractural arachnodactyly, respectively, highlights their critical contribution to connective tissue integrity (Ramirez, 1996).

Fibrillin molecules have a cysteine-rich multidomain organisation dominated by calcium-binding epidermal growth factor-like domains (cbEGF-like domains) interspersed with eight-cysteine-containing motifs (TB modules; Pereira et al., 1993; Zhang et al., 1994). The contiguous arrays of cbEGF-like domains form rod-like structures in the presence of calcium (Downing et al., 1996; Reinhardt et al., 1997). Each isoform contains a unique hydrophobic sequence towards the amino terminus which may act as a potential molecular hinge; in fibrillin-1 this sequence is proline-rich sequence, and in fibrillin-2 it is glycine-rich. Amino- and carboxy-terminal fibrillin sequences contain furin/PACE proprotein convertase tetrabasic consensus sequences, and processing at these sites may be important regulatory steps in fibrillin assembly (Raghunath et al., 1999; Ritty et al., 1999).

The molecular pathway of fibrillin assembly remains poorly understood. Intermediates have proved difficult to identify due to the large size of fibrillin molecules and their propensity to form disulphide-bonded aggregates (Sakai, 1990). The possibility that dimers may occur has been suggested by SDS-PAGE analysis of metabolically labelled fibrillin immunoprecipitated from cell culture medium (Kielty and Shuttleworth, 1993), and recent recombinant studies (Trask et al., 1999; Ashworth et al., 1999). Efforts have concentrated on resolving the precise arrangement of fibrillin monomers within microfibrils, in order to understand their structural properties and to gain insights into how they form. A parallel head-to-tail alignment model of unstaggered fibrillin monomers with amino- and carboxy-termini at, or close to, the beads was suggested on the basis of antibody epitope mapping and measured molecular dimensions (Reinhardt et al., 1996). Alternative staggered arrangements based on extrapolation of molecular length from cbEGF-like domain dimensions (Downing et al., 1996), or on alignment of transglutaminase cross-link sites (Qian and Glanville, 1998), have also been proposed.

In this study, we have investigated human fibrillin-1

assembly using a recombinant approach. We targetted the amino- and carboxy-terminal regions of the molecule because of their localisation at, or close to, the beads (Reinhardt et al., 1996), and the fact that extracellular furin processing of the carboxy terminus is apparently necessary for stable deposition of fibrillin (Raghunath et al., 1999). We have investigated whether these sequences interact specifically, and whether such interactions are influenced by carboxy-terminal furin processing. Our data demonstrate, for the first time, that amino-terminal polypeptides associate specifically with processed carboxy-terminal polypeptides. This overlapping molecular association could drive linear accretion of processed fibrillin molecules in the extracellular space.

MATERIALS AND METHODS

Fibrillin cDNA constructs

A fibrillin-1 carboxy-terminal cDNA clone (cFib-1) (Fig. 1) encoding exons 50-65 (nucleotides 6562 to 9035) (accession number 63556) was constructed from clone F3.4 (Pereira et al., 1993), as previously reported (Ashworth et al., 1999). The cFib-1 construct contained the RXRR furin consensus sequence in exon 64 (residues 2726-2731, Pereira et al., 1993), the intrinsic fibrillin-1 stop codon, and 24 nucleotides of the 3′ untranslated region.

Three mutant forms of cFib-1 were generated by site-directed mutagenesis (Stratagene, UK). The proximal N-glycosylation site (Asn-Glu-Thr, NET, residues 2734-2736, Pereira et al., 1993) of the carboxy terminus was mutated to QET, and this mutant clone was designated cFib-1^{NG1}. The second N-glycosylation site (NVS, residues 2750-2752) of cFib-$1^{NG1}$was then altered to QVS by site-directed mutagenesis of cFib-1^{NG1} to generate mutant cFib-1^{NG12}. The third N-glycosylation site of cFib-1^{NG12} (NIS, residues 2767-2769) was altered to QIS by site directed mutagenesis to generate mutant cFib-1^{NG123} (Fig. 1).

A fibrillin-2 carboxy-terminal clone (cFib-2) (Fig. 1) encoding exons 57-65 (nucleotides 7223-9008) was constructed from clone 3′9 (Zhang et al., 1994) by ligation at *Eco*RI and *Eco*RV sites into vector pSecTagB (Invitrogen). The cFib-2 clone contained the putative furin cleavage site DSRQKR (residues 2773-2778), the intrinsic fibrillin-2 stop codon, and 292 nucleotides of 3′ untranslated region.

A fibrillin-1 amino-terminal cDNA clone, nFib-1, encoding exons 1-15 (nucleotides 391-2358) (Fig. 1) was constructed from clone 5′F (Pereira et al., 1993), and subcloned into vector pSecTagA (Invitrogen) (Ashworth et al., 1999).

A truncated nFib-1, snFib-1, encoding exons 1-8 (nucleotides 391-1392) (Fig. 1) was constructed from nFib-1, and subcloned into pSecTagA.

A fibrillin-1 minigene, miniFib-1, corresponding to nFib-1 exons 1-15 (nucleotides 391 to 2355) ligated to cFib-1 exons 50-65 (nucleotides 6558-9035), was generated by ligation of nFib-1 and cFib-1 in vector pSecTagA (Fig. 1).

For the nFib-1, snFib-1 and mFib-1 constructs, the start ATG translation initiation codon within the vector was removed by site-directed mutagenesis, in order to utilise the intrinsic fibrillin-1 start codon.

A cDNA encoding a three-domain fibrillin-1 cDNA (complete exons 9-11; the first TB module, proline-rich region and EGF domain), designated profib-1, was generated by reverse transcriptase-polymerase chain reaction using human dermal fibroblast mRNA (Hindson et al., 1999). The profib-1 cDNA was subcloned into the mammalian expression vector pSecTag (Invitrogen).

All constructs and mutations, correct vector insertions and the exon 15-50 junction of mFib-1 were verified by dye-terminator automated sequencing.

In vitro transcription

The vectors containing cFib-1 and mFib-1 were linearised with 15 units of *Pme*I restriction enzyme (New England Biolabs). The cFib-1 and miniFib-1 constructs contained the intrinsic fibrillin-1 TAA stop codon at nucleotide 9009, at which translation of these constructs terminates. nFib-1 and snFib-1 were linearised with 15 units of *Apa*I restriction enzyme (Boehringer-Mannheim, UK), at a site within the pSecTag multiple cloning site. Linear DNA was transcribed by T7 RNA polymerase (Promega, UK), and purified RNA was heated to 60°C for 10 minutes before use to disrupt secondary structure.

Preparation of semi-permeabilised HT1080 cells

Semi-permeabilised HT1080 cells were prepared as previously described (Wilson et al., 1995; Lees et al., 1997; Ashworth et al., 1999). A 75 cm^3 flask of cells was grown to confluency (in Dulbecco's modified Eagle's medium with 10% fetal calf serum, 1% glutamine, 1% penicillin and streptomycin), trypsinised and resuspended in 8 ml of KHM buffer (20 mM Hepes, pH 7.2, containing 10 mM potassium acetate, 2 mM magnesium acetate) and 100 μg/ml soybean trypsin inhibitor, then pelleted at 10,000 ***g*** for 3 minutes. Cells were resuspended in 6 ml KHM buffer containing 40 μg/ml digitonin and incubated on ice for 5 minutes. KHM (8 ml) was added to terminate permeabilisation, then the cells were pelleted and resuspended in 11 ml of Hepes buffer (50 mM Hepes, pH 7.2, 90 mM potassium acetate). After 10 minutes, the cells were pelleted and resuspended in 100 μl KHM. Staphylococcal nuclease (10 μg/ml) and calcium chloride to a final concentration of 1 mM were added, and the cells were incubated at room temperature for 12 minutes. The reaction was terminated by adding EGTA to a final concentration of 4 mM.

In vitro translation in the presence of semi-permeabilised cells

Fibrillin RNA was translated in the presence of semi-permeabilised HT1080 cells as previously described (Ashworth et al, 1999) using rabbit reticulocyte lysate (Flexilysate, Promega, Southampton, UK) for 1.5 hours at 30°C. Each reaction contained 35 μl lysate, 1 μl RNase inhibitor (40 units/ml), 1 μl amino acids minus cysteine (1 mM), 1 μl potassium chloride (2.5 M), 3 μl ^{35}S cysteine (ICN Biomedicals Ltd, UK) (10 μCi/μl) and 2.5 μl prepared RNA.

This is a well characterised system that effectively recapitulates endoplasmic reticulum folding and post-translational modifications of molecules destined for secretion (Wilson et al., 1995; Lees et al., 1997). The apparent molecular masses of the wild-type recombinant molecules, as judged by SDS-PAGE analysis, were 75 kDa (nFib-1), 35 (snFib-1), 190 (miniFib-1), 110 (cFib-1), 22 kDa (profib-1) and 70 kDa cFib-2 (see Figs 2-6). All of these recombinant molecules except snFib-1, which contains no N-glycosylation sites, were N-glycosylated as judged by increased electrophoretic mobility following endoglycosidase H treatment, as previously shown (Ashworth et al., 1999). Mutant cFib-1^{NG} molecules, which have N-glycosylation sites knocked out, migrated slightly faster than cFib-1, confirming reduced N-glycosylation (see Fig. 3B).

Carboxy-terminal processing of fibrillin-1 by furin-type protease

Translations of wild-type cFib-1, mutant cFib-1 molecules, miniFib-1 or cFib-2, and co-translations of cFib-1 with nFib-1, and cFib-1 with snFib-1, were carried out in the presence of semi-permeabilised HT1080 cells. The cells were then pelleted, washed twice with KHM buffer, then lysed in 10 μl resuspension buffer (50 mM Tris-HCl, pH 7.4, 150 mM sodium chloride, 1% Triton X-100) on ice for 10 minutes. Calcium chloride (to 5 mM) and resuspension buffer without Triton X-100 were added to a final volume of 20 μl, and the reaction incubated for 2 to 18 hours at 4°C or 37°C (Ashworth et al., 1999). Some incubations were carried out in the absence or presence of the selective furin inhibitor decanoyl-Arg-Val-Lys-Arg (R-V-K-R)-chloromethylketone (DCK) (Bachem, Switzerland) to a final

concentration of 13 mM, or EGTA to a final concentration of 40 mM, or PMSF to a final concentration of 10 mM (Ashworth et al., 1999).

Size fractionation of recombinant fibrillin

cFib-1, miniFib-1, cFib-1 cotranslated with nFib-1, and cFib-1 with snFib-1, were allowed to undergo carboxy-terminal processing by furin-type protease activity at 37°C for 18 hours, as described above. Reaction volumes were then made up to 100 μl with immunoprecipitation buffer. Samples were centrifuged twice at 13,000 rpm for 10 minutes to remove cellular debris. Size fractionation of non-reduced ^{35}S-labelled fibrillin was carried out on an AKTA Purifier system using a Superdex 200 PC 3.2/30 column (volume 2.4 ml, fraction size 50 μl) in buffer (50 mM Tris-HCl, pH 7.4, containing 150 mM sodium chloride). This system allows accurate and reproducible separation of molecules and assembly intermediates under non-denaturing and non-reducing conditions. The Superdex 200 column was calibrated using proteins of known molecular mass which were thyroglobulin (669 kDa), albumin (67 kDa), ovalbumin (43 kDa), chymotrypsin (25 kDa) and ribonuclease (13.7 kDa).

SDS-PAGE analysis and autoradiography

An equal volume of SDS-PAGE loading buffer was added to each labelled translation product. Samples were boiled for 5 minutes in the presence or absence of 50 mM DTT, prior to loading on 6%, 8% or 15% SDS-PAGE gels. After electrophoresis, gels were fixed in 10% glacial acetic acid, 25% industrial methylated spirit, briefly washed in distilled water and dried under vacuum. Gels were visualised by autoradiography using Kodak Biomax MR film.

Co-immunoprecipitation of carboxy-terminal fibrillin with calreticulin

Cross-linking and immunoprecipitation was performed as previously described (Wilson et al., 1995). Translations of cFib-1 and cFib-1^{NG1} were carried out in the presence of semi-permeabilised cells and terminated by the addition of cycloheximide to 1 mM. The cells were pelleted, washed and resuspended in 50 μl KHM buffer. Dithiobis succinimydylpropionate (DSP) (a reducible cross-linker of primary amines such as the lysine side chain) (Pierce and Warriner Ltd, UK) was added to 1 mM and the reaction incubated at 25°C for 10 minutes. Cross-linking with DSP was terminated by addition of glycine to 2 mM and incubation at 25°C for 10 minutes. Samples were boiled for 5 minutes in an equal volume of denaturation buffer (25 mM Tris-HCl, pH 7.5, 150 mM sodium chloride, 1% w/v SDS, 1% v/v Nonidet P-40) and centrifuged at 13,000 rpm for 10 minutes. The supernatant was adjusted to a final volume of 1 ml in immunoprecipitation buffer (50 mM Tris-HCl, pH 7.4, 150 mM sodium chloride, 10 mM EDTA, 1% v/v Triton X-100). Samples were precleared by addition of 50 μl of Protein A Sepharose (10% w/v in PBS) and incubation at 4°C for 40 minutes. Samples were centrifuged at 10,000 rpm for 1 minute and the supernatant adjusted to 1 ml with immunoprecipitation buffer. Rabbit anti-calreticulin polyclonal antibody (StressGen Biotechnologies Corp., York, UK) was added to the sample at a 1 in 400 dilution with 50 μl of Protein A Sepharose (10% w/v in PBS) and incubated at 4°C for 18 hours. Samples were pelleted by centrifugation at 13,000 rpm for 30 seconds and the pellet washed twice in immunoprecipitation buffer, once in immunoprecipitation buffer with 500 mM sodium chloride and once in immunoprecipitation buffer alone. SDS-PAGE loading buffer was added with 50 mM DTT and samples boiled for 5 minutes. The samples were spun at 13,000 rpm for 30 seconds and the supernatant loaded onto SDS-PAGE gels.

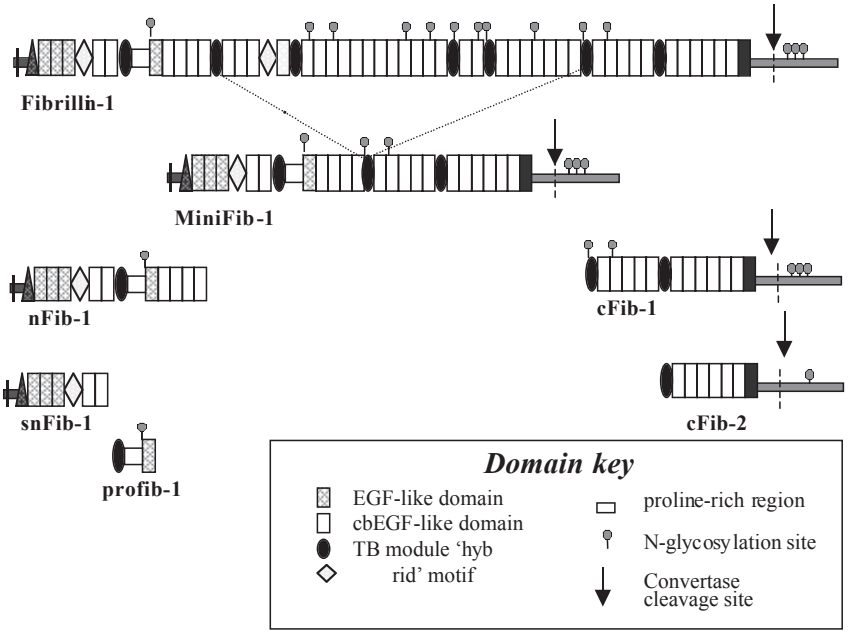

Fig. 1. Fibrillin constructs. Human fibrillin-1 and fibrillin-2 cDNAs encoding the recombinant molecules used in this study (see Materials and Methods). They were amino-terminal fibrillin-1 molecules (nFib-1 and snFib-1), an carboxy-terminal fibrillin-1 molecule (cFib-1), a three-domain peptide from fibrillin-1 (profib-1), and a minigene fibrillin-1 (miniFib-1).

RESULTS

Carboxy-terminal furin-mediated processing of fibrillin-1 and fibrillin-2 molecules occurs downstream from the endoplasmic reticulum

We have previously shown that translocated cFib-1 molecules generated in the in vitro translation system supplemented with semi-permeabilised cells do not undergo carboxy-terminal processing at the furin-type protease site (Ashworth et al., 1999). However, removal of ~20 kDa of carboxy-terminal sequence can be induced experimentally in cFib-1 and miniFib-1 by lysing the washed cells then incubating the cell lysates at 37°C (Fig. 2A-C, see also Fig. 3). This processing is mediated by furin-type proteases, since it is calcium dependant, and inhibited by PMSF and the selective furin inhibitor DCK (Raghunath et al., 1999; Ashworth et al., 1999). In these experiments, the fibrillin-2 carboxy-terminal polypeptide, cFib-2, has been shown for the first time also to undergo furin-mediated processing after cell lysis, although this processing was much less efficient than for cFib-1 under identical experimental conditions (Figs 2D, 3B).

Potential furin-type processing of the amino-terminal fibrillin-1 polypeptides nFib-1 and snFib-1, predicted to remove the first ~eighteen amino acids following the signal peptide, could not be detected electrophoretically.

Influence of N-glycosylation on carboxy-terminal fibrillin processing

Recent studies have highlighted that carboxy-terminal processing of fibrillin is a prerequisite for extracellular

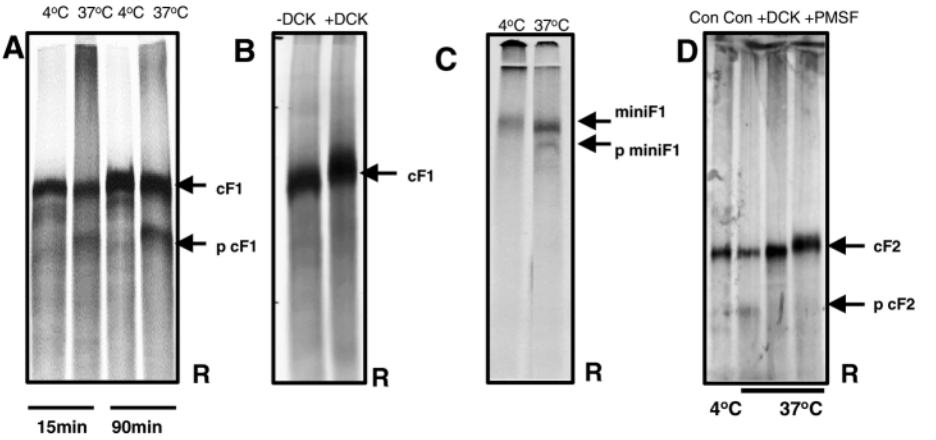

Fig. 2. Electrophoretic analysis of cFib-1 furin processing. cFib-1 and cFib-2 were translated in a cell-free translation system supplemented with semi-permeabilised cells (see Materials and Methods). The cells were then lysed, and incubated at either 4°C or 37°C for 16 hours, in order for processing to occur (Ashworth et al., 1999). DCK and PMSF both inhibit furin-type proteases, and both were shown to inhibit fibrillin processing. (A) cFib-1 (cF1)-containing cell lysates were incubated at 4°C or 37°C for 15 minutes or 90 minutes. After 90 minutes, a proportion of cF1 had been processed with loss of ~20 kDa. (B) cF1-containing cell lysates were incubated at 4°C, or treated with DCK at 37°C. In neither case, did processing occur. (C) MiniFib-1 (miniF1)-containing cell lysates were incubated at 4°C or 37°C. When treated at 37°C, processing with loss of ~20 kDa was observed. (D) cFib-2 (cF2)-containing cell lysates were incubated at 37°C for 16 hours. A small proportion of moelcules were processed with loss of ~20 kDa. When incubated in the presence of DCK or PMSF, no processing was observed.

deposition (Raghunath et al., 1999). In order to investigate whether N-glycosylation of the three N-glycosylation sites within exons 64/65 downstream of the furin-type protease cleavage site influences this crucial carboxy-terminal cleavage event, three constructs were generated in which these N-glycosylation sites were consecutively knocked out by site-directed mutagenesis of each N residue (cFib-1^{NG1}, cFib-1^{NG12} and cFib-1^{NG123}) (Fig. 3).

Removal of the adjacent N-glycosylation site three residues downstream from the fibrillin-1 furin consensus sequence (cFib-1^{NG1}) markedly increased the proportion of molecules that were cleaved relative to wild-type cFib-1 under identical experimental conditions (Fig. 3A). Densitometric analysis of reduced samples revealed that, after 18 hours at 37°C, 60-63% of cFib-1 was processed whereas 78-80% of cFib-1^{NG1} was processed. Removal of the two subsequent downstream N-glycosylation sites had little effect on efficacy of processing (Figs 3B, 4B, not shown). An additional band migrating slightly faster than cFib-1 was apparent in some experiments (Fig. 3B tracks 1, 2; Fig. 4B, tracks 1, 3). This band could be newly-translocated unglycosylated cFib-1, or may indicate the presence of a secondary cleavage site within the carboxy terminus.

These data indicate a key role for the N-glycosylation site that lies immediately downstream of the carboxy-terminal furin cleavage site in regulating this crucial processing event.

Regulation of fibrillin-1 carboxy-terminal processing by chaperones

The possibility that an association of molecular chaperones, either directly with the unprocessed cFib-1 molecule or with N-linked carbohydrates at the carboxy terminus, might influence furin cleavage, was investigated. cFib-1 was found to co-immunoprecipitate with calreticulin (48 kDa), protein disulphide isomerase (PDI) (58 kDa), and BiP (78 kDa) after DSP cross-linking (Fig. 4A). No processing occurred when cFib-1, cFib-1^{NG1} and cFib-1^{NG12} were cross-linked with DSP prior to cell lysis (Fig. 4B). In these experiments, the unprocessed DSP-treated cFib-1 and mutant cFib-1 molecules migrated slightly slower than untreated control molecules. In addition, a higher molecular mass band (~140 kDa) was present in the cross-linked cFib-1 and cFib-1^{NG1} samples, but not cFib-1^{NG12}. The size of this band is consistent with the

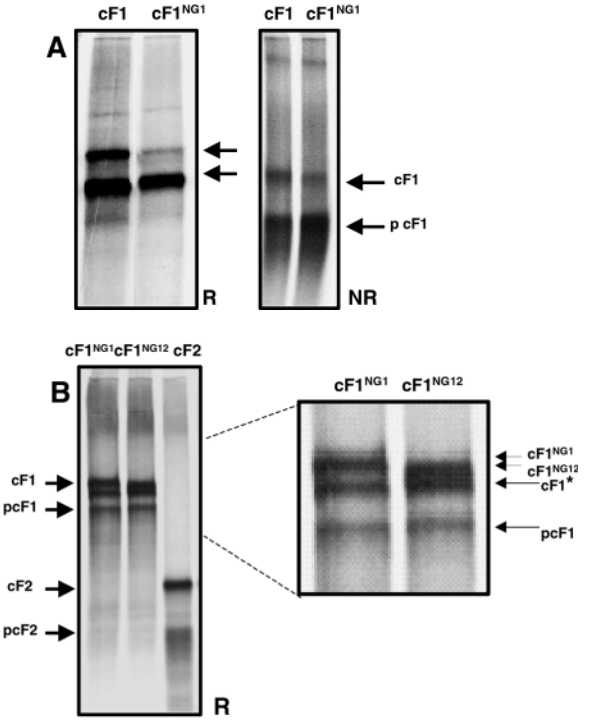

Fig. 3. Electrophoretic analysis of mutant cFib-1 furin processing. cFib-1, mutant cFib-1 molecules with N-glycosylation sites knocked out (cFib-1^{NG1}, cFib-1^{NG12}) and cFib-2 were translated in a cell-free translation system supplemented with semi-permeabilised cells (see Materials and Methods). The cells were then lysed, and incubated at either 4°C or 37°C for 16 hours, in order for processing to occur (Ashworth et al., 1999). (A) cFib-1 (cF1) and $cF1^{NG1}$-containing cell lysates were incubated at 37°C for 16 hours. Mutant molecules were almost completely processed, in contrast to wild-type molecules. (B) cF1 and $cF1^{NG12}$-containing cell lysates were incubated at 37°C for 16 hours. Processing of mutant $cF1^{NG12}$ was similar to that of wild-type molecules. In comparison, when cFib-2 (cF2)-containing cell lysates were incubated at 37°C for 16 hours, only a small proportion of molecules were processed with loss of ~20 kDa.

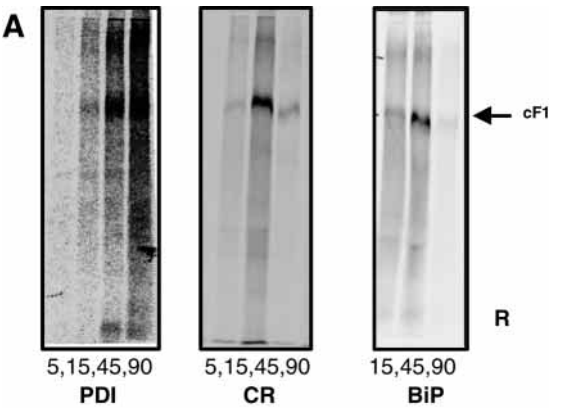

Fig. 4. Chaperone associations with cFib-1. cFib-1, cF1^{NG1} and cF1^{NG12} molecules were each translated in a cell-free translation system supplemented with semi-permeabilised cells (see Materials and Methods). The cells were then lysed, and incubated at 37°C for 16 hours, in order for processing to occur (Ashworth et al., 1999). (A) When cFib-1 (cF1) was cross-linked with the reducible cross-linker DSP, it co-immunoprecipitated with protein disulphide isomerase (PDI), calreticulin (CR) and BiP. Incubation times (15, 30, 45 and 90 minutes) are indicated. (B) cF1 and mutants were not processed following cross-linking with DSP. A higher-molecular mass band of ~140 kDa was also apparent in cF1 and cF1^{NG1}samples after DSP cross-linking. (C) Following DSP cross-linking, calreticulin antiserum prominently co-immunoprecipitated the unprocessed form of cF1, but only a faint trace of processed cF1 was detected.

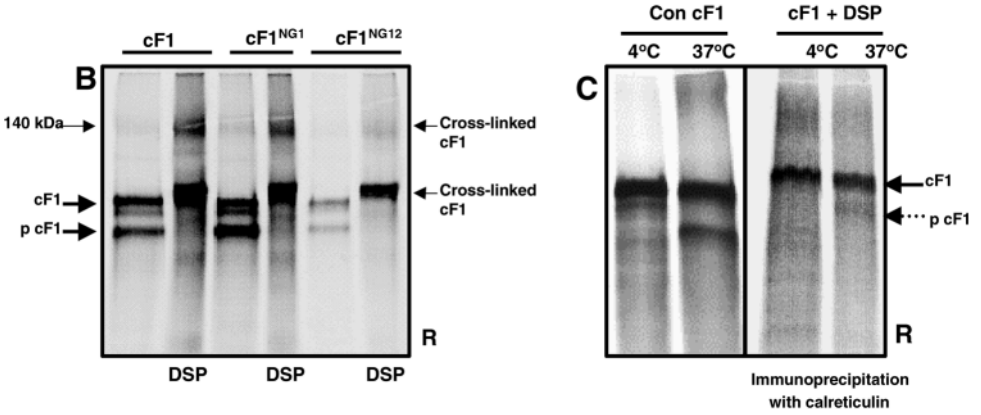

association of cFib-1 (90 kDa) with calreticulin but not with PDI or BiP. When unprocessed plus processed wild-type cFib-1 present in cell lysates were subjected to co-immunoprecipitation with calreticulin after DSP cross-linking, the unprocessed form was prominently associated with calreticulin compared to only traces of the processed form (Fig. 4C). When unprocessed and processed cFib-1^{NG1} was coimmunoprecipitated with anti-calreticulin antiserum after DSP cross-linking, unprocessed molecules were detected even though the majority of the cFib-1^{NG1} molecules present were processed (not shown). Cross-linking itself did not inhibit furins as judged by the fact that DSP-treated HT1080 cell lysates retained their ability to process cFib-1 generated by cell-free translation (not shown). These data suggest that chaperones are associated with the carboxy terminus of cFib-1, and that their association may inhibit furin processing.

Aggregation of amino- and carboxy-terminal fibrillin-1

Size fractionation of recombinant fibrillin molecules was undertaken in non-denaturing and non-reducing conditions as an assay of molecular associations (Figs 5, 6). Size fractionation of cFib-1 and miniFib-1 was carried out on samples from lysed cells that contained both unprocessed and processed forms.

A small proportion of unprocessed cFib-1 molecules eluted in the void volume, but in contrast, the processed form did not aggregate (Fig. 5A). When miniFib-1 was size fractionated, unprocessed and processed molecules were both present in the void volume fractions (Fig. 5B). Size fractionation of nFib-1 (Fig. 5C) and snFib-1 (not shown) revealed that both these amino-terminal fibrillin-1 molecules formed abundant high-molecular mass disulphide bonded aggregates.

When nFib-1 and cFib-1 were co-translated prior to incubation of washed cell lysates for 2 or 16 hours at 37°C to allow furin-type processing, it was apparent that the proportion of processed to unprocessed cFib-1 was increased, and that processed molecules were now present in high-molecular mass aggregates that eluted in the void volume (Fig. 6A,B). When snFib-1 (Fig. 6C) or profib-1 (Fig. 6D) were substituted for nFib-1, processed cFib-1 was no longer detected in the void volume fractions.

These experiments highlight that the extreme carboxy-terminal sequence of fibrillin-1 downstream of the furin cleavage site is capable of molecular association, and that processed carboxy-terminal molecules do not aggregate unless amino-terminal exons 11-15 are present.

DISCUSSION

By analogy with linear structural extracellular matrix polymers such as collagen fibres, which form in the extracellular space by tightly regulated self-assembly processes driven by primary structure (Kielty et al., 1993), the formation of fibrillin-rich microfibrils may be initiated by linear self-assembly of the fibrillin scaffold. However, despite intensive study the molecular interactions that drive linear fibrillin assembly in the extracellular space have eluded definition. Early studies focussed on elucidating the alignment of fibrillin molecules in microfibrils, and immunolocalisation of fibrillin epitopes suggested a parallel head-to tail arrangement (Sakai et al., 1991). More recently, a ~35% staggered alignment of fibrillin molecules in microfibrils was indicated following identification of transglutaminase cross-links in fibrillin-1 extracted from human amnion (Qian and Glanville, 1998). The unidirectional axial nature of untensioned microfibrils was established by STEM mass mapping and atomic force microscopy, supporting a parallel arrangement of fibrillin molecules (Hanssen et al., 1998; Sherratt et al., 1999). Key questions that remain are precisely how fibrillin molecules

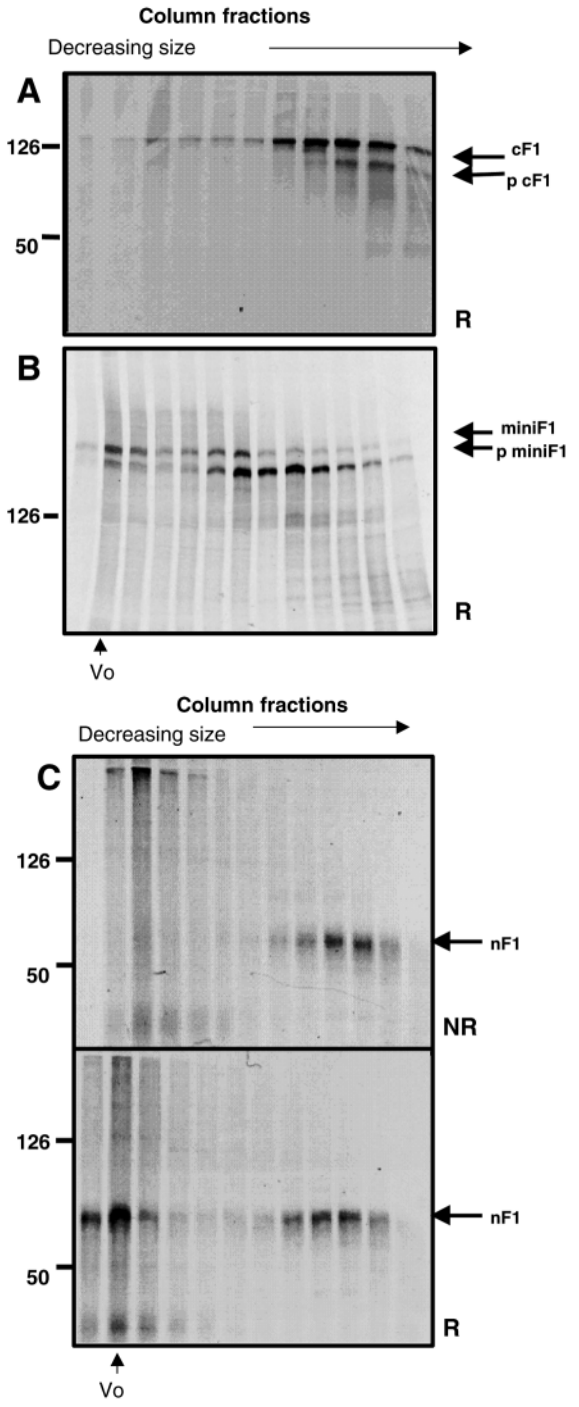

Fig. 5. Electrophoretic analysis of nFib-1, cFib-1 and miniFib-1 after size fractionation. nFib-1, cFib-1 and miniFib-1 molecules were each translated in a cell-free translation system supplemented with semi-permeabilised cells (see Materials and Methods). The cells were then lysed, and incubated at 37°C for 16 hours, in order for processing to occur (Ashworth et al., 1999). cFib-1 (A), miniFib-1 (B) and nFib-1 (C) were size fractionated in non-reducing conditions on an AKTA Purifier System using a Superdex 200 PC 3.2/30 column equilibrated in 0.05 M Tris-HCl, 0.15 M NaCl. Column fractions were then run on 8% SDS-PAGE gels in the absence or presence of 50 mM dithiothreitol. nFib-1 formed abundant disulphide-bonded aggregates. Some unprocessed cFib-1, but not processed cFib-1, eluted in the void volume. Some processed and unprocessed miniFib-1 eluted in the void volume.

interact in the extracellular space to form periodic linear polymers and how cells prevent assembly from occurring intracellularly. Important clues have recently emerged that indicate a central regulatory role for carboxy-terminal furin-type protease processing in microfibril assembly. Irreversible inhibition of the carboxy-terminal conversion of 'profibrillin' to 'fibrillin' at the basic amino acid recognition sequence R-G-R-K-R-R for proprotein convertases of the furin/PACE family, and a mutation (R2726W) that replaces the P6 arginine in the cleavage site, inhibited fibrillin incorporation into the extracellular matrix (Raghunath et al., 1999).

Early biosynthetic and extraction studies indicated that newly-secreted fibrillin is rapidly incorporated into an extensive, disulphide bonded fibrillar network (Gibson et al., 1989; Sakai, 1990). Difficulties in electrophoretic resolution of full length fibrillin molecules and a tendency to form disulphide bonded aggregates have precluded characterisation of assembly intermediates, but also predict the existence of specific molecular recognition events that direct the correct alignment of newly secreted fibrillin molecules. In the present study, we used a recombinant approach to investigate amino- and carboxy-terminal molecular associations that might be important in linear assembly, and the role of carboxy-terminal processing in regulating such interactions. A mammalian expression system was chosen that rapidly generated ^{35}S-labelled N-glycosylated molecules that were folded and capable of binding calcium (Ashworth et al., 1999), that provided a means of generating unprocessed and furin-type protease cleaved molecules, and that permitted analysis of chaperone associations and their potential involvement in regulation of this processing. A size fractionation strategy was used to monitor fibrillin-1 molecular interactions, and the role and regulation of carboxy-terminal processing in such molecular associations.

The crucial importance of carboxy-terminal furin processing for amino- and carboxy-terminal fibrillin-1 interactions led us to examine the regulation of this processing event and, in particular, the putative involvement of the three N-glycosylation sites downstream of the furin cleavage site. Three mutant cFib-1 molecules were created that had one, two or all three N-glycosylation sites within the extreme carboxy-terminal sequence, knocked out. It was of particular interest to determine whether the N-glycosylation site just three residues downstream of the furin site influenced cleavage, and whether removal of the two downstream N-glycosylation sites had any additional effects on furin cleavage as a result of steric hindrance or chaperone associations. Removal of the N-glycosylation site immediately downstream of the furin site increased cleavage efficiency significantly, but the additional removal of the other two downstream sites had no effect. The presence of N-linked carbohydrate at the site adjacent to the cleavage sequence may thus be physiologically crucial in regulating the rate of pericellular fibrillin-1 assembly. Interestingly, fibrillin-2 contains only a single N-glycosylation site within the extreme carboxy terminus, which corresponds to the most carboxy-terminal site of fibrillin-1 (Zhang et al., 1994). Since fibrillin-2 has no N-glycosylation site immediately downstream from its predicted furin cleavage site, it might have been expected to undergo furin-driven processing more efficiently than fibrillin-1. However, carboxy-terminal furin processing of fibrillin-2, reported here for the first time,

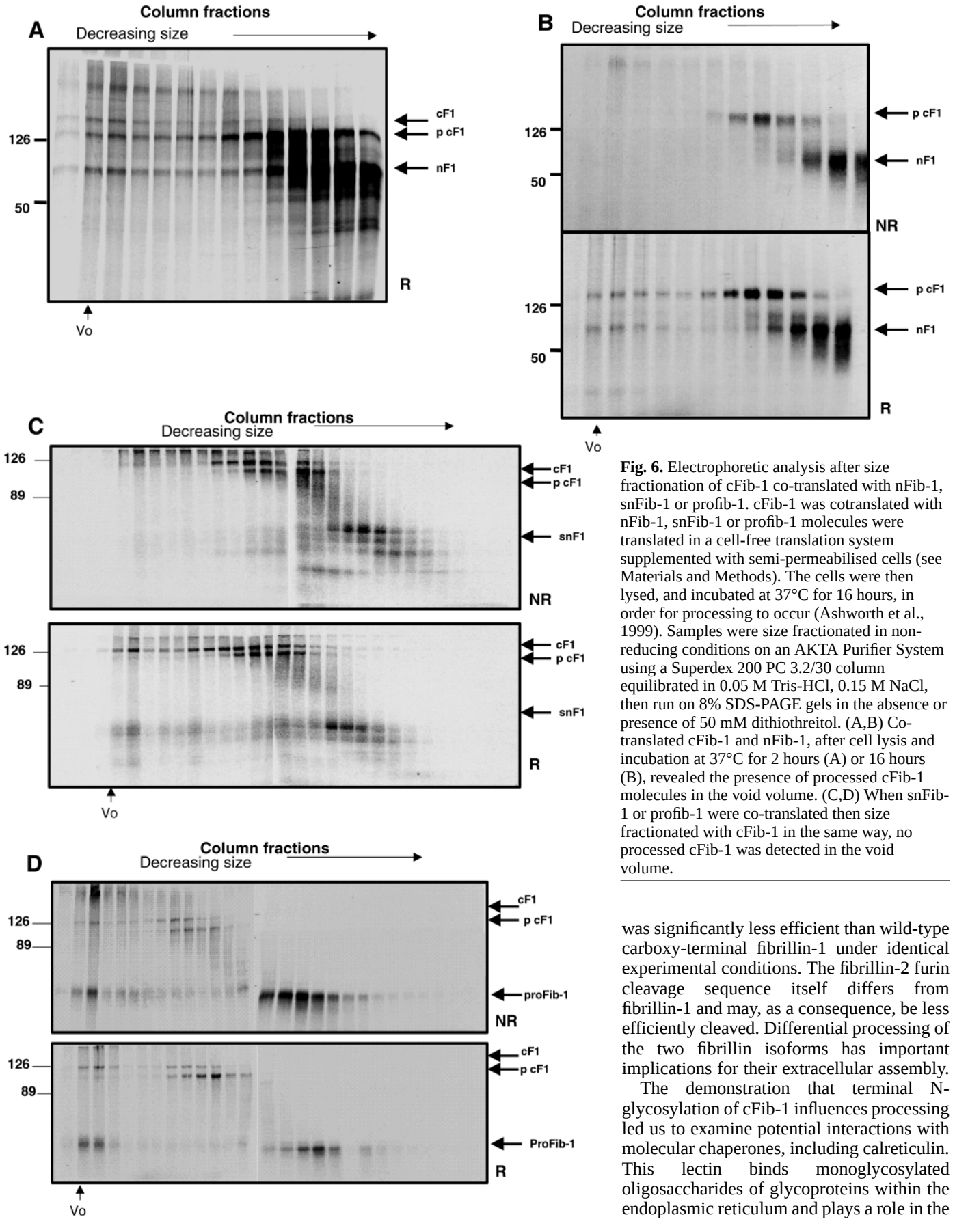

Fig. 6. Electrophoretic analysis after size fractionation of cFib-1 co-translated with nFib-1, snFib-1 or profib-1. cFib-1 was cotranslated with nFib-1, snFib-1 or profib-1 molecules were translated in a cell-free translation system supplemented with semi-permeabilised cells (see Materials and Methods). The cells were then lysed, and incubated at 37°C for 16 hours, in order for processing to occur (Ashworth et al., 1999). Samples were size fractionated in non-reducing conditions on an AKTA Purifier System using a Superdex 200 PC 3.2/30 column equilibrated in 0.05 M Tris-HCl, 0.15 M NaCl, then run on 8% SDS-PAGE gels in the absence or presence of 50 mM dithiothreitol. (A,B) Co-translated cFib-1 and nFib-1, after cell lysis and incubation at 37°C for 2 hours (A) or 16 hours (B), revealed the presence of processed cFib-1 molecules in the void volume. (C,D) When snFib-1 or profib-1 were co-translated then size fractionated with cFib-1 in the same way, no processed cFib-1 was detected in the void volume.

was significantly less efficient than wild-type carboxy-terminal fibrillin-1 under identical experimental conditions. The fibrillin-2 furin cleavage sequence itself differs from fibrillin-1 and may, as a consequence, be less efficiently cleaved. Differential processing of the two fibrillin isoforms has important implications for their extracellular assembly.

The demonstration that terminal N-glycosylation of cFib-1 influences processing led us to examine potential interactions with molecular chaperones, including calreticulin. This lectin binds monoglycosylated oligosaccharides of glycoproteins within the endoplasmic reticulum and plays a role in the

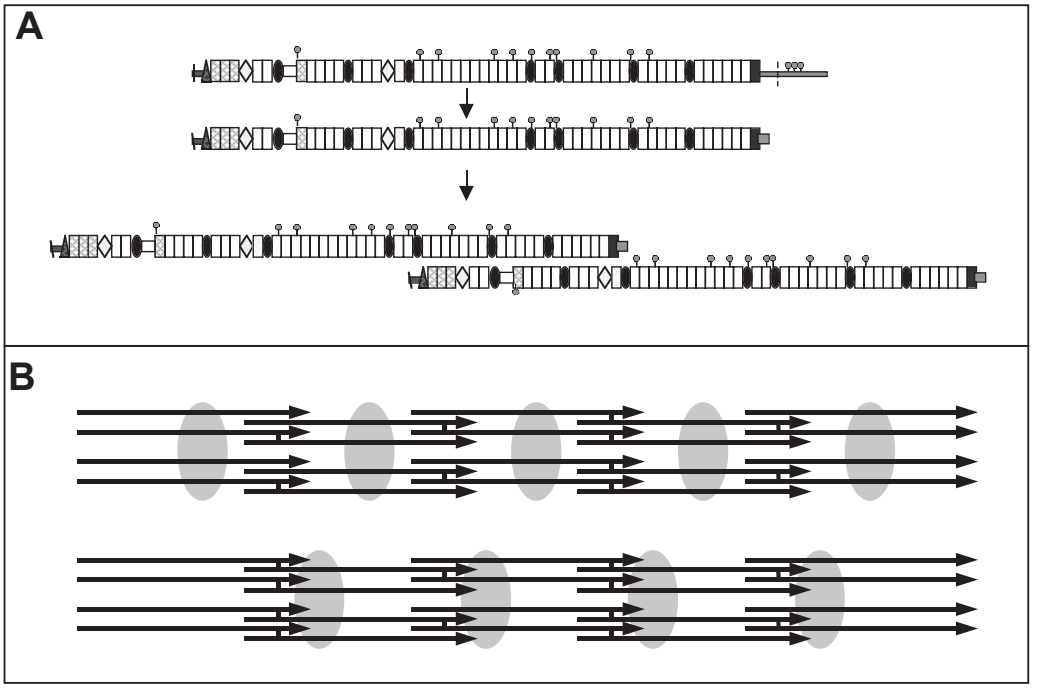

Fig. 7. Model of fibrillin alignment based on the processing and size fractionation data. (A) Domain structure diagram showing the predicted sequence of events in the linear assembly of fibrillin-1. Full-length fibrillin-1 molecules are pericellularly processed at the carboxy terminus, with removal of ~20 kDa. This processing event facilitates parallel alignment and association of overlapping amino- and carboxy-terminal sequences. Subsequently, transglutaminase cross-links, as previously reported (Qian and Glanville, 1997), may form that stabilise these linear fibrillin-1 arrays. (B) Line diagram model of the association of fibrillin-1 molecules in microfibrils. Fibrillin-1 dimers may be intermediates of assembly (see Ashworth et al., 1999; Trask et al., 1999). Overlapping parallel fibrillin-1 dimers (horizontal arrows) may be stabilised by transglutaminase cross-links (vertical lines), as shown above. The number of molecules in a microfibril cross-section, and both the composition and position of the 'beads' along the fibrillin-1 molecule, remain to be defined. Two potential bead locations consistent with current data are highlighted.

folding and assembly of molecules destined for secretion. Calreticulin has also been detected at cell surfaces (Arosa et al., 1999), and it plays an important role in cell, extracellular matrix interactions. Phosphorylation/dephosphorylation, dependent interactions of calreticulin and integrins such as $\alpha 3\beta 1$ lead to modulation of integrin-mediated transmembrane signalling (Coppolino and Dedhar, 1999). Using a cross-linking and immunoprecipitation strategy, we have shown here, for the first time, that unprocessed cFib-1 interacts very strongly with calreticulin, as well as with other chaperones that may also play a role in regulating processing. The interaction with calreticulin appears to be predominantly with the carboxy-terminal sequence, since only trace amounts of calreticulin were detected in association with processed cFib-1 molecules which still contain two upstream N-gycosylation sites (see Fig. 1). Cross-linking and co-immunoprecipitation experiments also showed that, even after removal of the N-glycosylation site immediately downstream of the furin cleavage site, some bound calreticulin remained associated with cFib-1. This association may be with the remaining carboxy-terminal N-linked carbohydrates, and/or directly with the terminal peptide sequence itself. These results suggest that calreticulin may play an important role in regulating processing, and/or influencing the subsequent fate of the carboxy-terminal peptide.

Size fractionation in native non-reducing conditions prior to SDS-PAGE highlighted that unprocessed, but not processed, carboxy-terminal fibrillin-1 (cFib-1) molecules could form high-molecular mass aggregates. Thus, the processed molecules do not possess specific molecular recognition and interaction sequences whereas the sequence downstream of the furin-type protease cleavage site contains a recognition sequence that mediates molecular association. Only a proportion of the unprocessed molecules associated, indicating that cellular mechanisms such as chaperone interactions probably limit this association intracellularly. The formation of abundant disulphide-bonded aggregates of amino-terminal fibrillin-1 (nFib-1) molecules indicates that this sequence contains key molecular recognition sequences. Following association, amino-terminal disulphide bonding could involve the unpaired cysteine residues of the first 'hybrid' TB module which contains nine cysteines and/or disulphide exchange between TB modules (Yuan et al., 1997). Recently, we and others have shown that recombinant amino-terminal fibrillin-1 polypeptides that contain the proline-rich region can dimerise; this specific association may contribute to these amino-terminal aggregation events (Ashworth et al., 1999; Trask et al., 1999). It remains unclear whether monomers or dimers are the fundamental intermediate of microfibril assembly, or whether dimers represent an alternative extracellular form of fibrillin.

In vitro cotranslation of nFib-1 plus cFib-1 indicated for the first time that processed cFib-1 is able to associate with the amino-terminal sequence of fibrillin-1. These experiments suggest that processed fibrillin-1 molecules can interact in a staggered overlap (assuming a parallel alignment) and that this arrangement could form the basis of linear assembly of processed fibrillin in the extracellular space (Fig. 7). Further cotranslation experiments localised, to exons 12-15, the amino-terminal sequence that recognises processed carboxy-terminal fibrillin-1 molecules. This sequence overlaps with the predicted amino-terminal transglutaminase site identified by Qian and Glanville (1998); the carboxy-terminal molecules utilised in these experiments also contained the predicted carboxy-terminal cross-link site. Together, these data suggest

that the amino-terminal cross-link site falls within exons 14 and 15 which encode two contiguous cbEGF-like domains. Since exon 14 contains three lysines (residues 595, 599 and 612) and a single glutamine (residue 603), but exon 15 contains neither residue, exon 14 is probably the amino-terminal transglutaminase cross-link site. We were unable to distinguish unprocessed and furin processed nFib-1 electrophoretically, and it is unclear whether amino-terminal processing is also a prerequisite for assembly.

These studies have provided important new insights into fibrillin assembly. We have highlighted molecular amino- and carboxy-terminal interactions that depend upon carboxy-terminal processing furin-processed fibrillin-1 molecules, and which could allow linear accretion of fibrillin in the extracellular space. We have also demonstrated the crucial role of the N-glycosylation site of fibrillin-1 adjacent to the carboxy-terminal cleavage sequence in regulating processing, and a key interaction with calreticulin which may have physiological significance beyond a molecular chaperoning role.

This work was funded by the Medical Research Council UK (C.M.K.) and by a Wellcome Trust Vision Science Fellowship award (J.L.A.). The profib-1 cDNA was prepared by Ms S. Cunliffe, and site-directed mutagenesis of N-glycosylation consensus sequences by Mr D. Elks.

REFERENCES

Arosa, F. A., deJesus, O., Porto, G., Carmo, A. M. and deSousa, M. (1999). Calreticulin is expressed on the cell surface of activated human peripheral blood T lymphocytes in association with major histocompatibility complex class I molecules. *J. Biol. Chem.* **274**, 16917-16922.

Ashworth, J. L., Murphy, G., Rock, M.. J., Sherratt, M. J., Shapiro, S. D., Shuttleworth, C. A. and Kielty, C. M. (1999). Fibrillin degradation by matrix metalloproteinases: implications for connective tissue remodelling. *Biochem. J.* **340**, 171-181.

Coppolino, M. G. and Dedhar, S. (1999). Ligand-specific, transient interaction between integrins and calreticulin during cell adhesion to extracellular matrix proteins is dependent upon phosphorylation/ dephosphorylation events. *Biochem. J.* **340**, 41-50.

Downing, A. K., Knott, V., Werner, J. M., Cardy, C., Campbell, I. D. and Handford, P. A. (1996). Solution structure of a pair of calcium-binding epidermal growth factor-like domains of fibrillin-1, the Marfan gene product. *Cell* **85**, 597-605.

Gibson, M. A., Kumaratilake, J. S. and Cleary, E. G. (1989). The protein components of the 12-nanometer microfibrils of elastic and non-elastic tissues. *J. Biol. Chem.* **264**, 4590-4598.

Hanssen, E., Franc, S. and Garrone, R. (1998). Atomic force microscopy and modeling of natural elastic fibrillin polymers. *Biol. Cell* **90**, 223-228.

Hindson, V. J., Ashworth, J. L., Rock, M. J., Cunliffe, S., Shuttleworth, C. A. and Kielty, C. M. (1999). Fibrillin degradation by matrix metalloproteinases: identification of amino- and carboxy-terminal cleavage sites. *FEBS Lett.* **452**, 195-198.

Kielty, C. M. and Shuttleworth, C. A. (1993). Synthesis and assembly of fibrillin by fibroblasts and smooth muscle cells. *J. Cell Sci.* **106,** 167-173.

Kielty, C. M., Hopkinson, I. and Grant, M. E. (1993). The collagen family: structure, assembly and organisation in the extracellular matrix. In *Connective Tissue and its Heritable Disorders* (ed. P. M. Royce and B. Steinmann), pp 103-147. New York: Wiley Liss.

Kielty, C. M. and Shuttleworth, C. A. (1995). Fibrillin-containing microfibrils: structure and function in health and disease. *Int. J. Biochem. Cell Biol.* **27**, 747-760.

Lees, J. F., Tasab, M. and Bulleid, N. J. (1997). Identification of the molecular recognition sequence which determines the type-specific assembly of procollagen. *EMBO J.* **16**, 908-916.

Mecham, R. P. and Heusar, J. E. (1991). The elastic fiber. In *Cell Biology of the Extracellular Matrix* (ed. E. D. Hay), pp. 79-109. Plenum Press, New York..

Pereira, L., D'Alessio, M., Ramirez, F., Lynch, J. R., Sykes, B., Pangilinan, T. and Bonadio, J. (1993). Genomic organisation of the sequence coding for fibrillin-1, the defective gene product in Marfan syndrome. *Hum. Mol. Genet*. **2**, 961-968.

Qian, R. Q. and Glanville, R. W. (1997). Alignment of fibrillin molecules in elastic microfibrils is defined by transglutaminase-derived cross-links. *Biochemistry* **36**, 15841-15847.

Raghunath, M., Putnam, E. A., Ritty, T., Hamstra, D., Park, E-S., Tschödrich-Rotter, M., Peters, R., Rehemtulla, A. and Milewicz, D. M. (1999). Carboxy-terminal conversion of profibrillin to fibrillin at a basic site by PACE/furin-like activity required for incorporation in the matrix. *J. Cell Sci*. **112**, 1093-1100.

Ramirez, F. (1996). Fibrillin mutations and related phenotypes. *Curr. Opin. Genet. Dev.* **6**, 309-315.

Reinhardt, D. P., Keene, D. R., Corson, G. M., Pöschl, E., Bachinger, H. P., Gambee, J. E. and Sakai, L. Y. (1996). Fibrillin-1: organisation in microfibrils and structural properties. *J. Mol. Biol*. **258**, 104-116.

Reinhardt, D. P., Mechling, D. E., Boswell, B. A., Keene, D. R., Sakai, L. Y. and Bachinger, H. P. (1997). Calcium determines the shape of fibrillin. *J Biol. Chem.* **272**, 7368-7373.

Ritty, T., Broekelmann, T., Tisdale, C., Milewicz, D. M. and Mecham, R. P. (1999). Processing of the fibrillin-1 carboxy-terminal domain. *J. Biol. Chem.* **274**, 8933-8940.

Sakai, L. Y. (1990). Disulphide bonds crosslink molecules of fibrillin in the connective tissue space. In *Elastin: Chemical and Biological Aspects* (ed. A. Tamburro and J. M. Davidson), pp. 213-227. Congedo Editore, Galatina, Italy.

Sakai, L. Y. Keene, D. R., Glanville, R. W. and Bachinger, H. P. (1991). Purification and partial characterisation of fibrillin, a cysteine-rich structural component of connective tissue microfibrils. *J. Biol. Chem*. **266**, 14763-14770.

Sherratt, M. J., Wess, T. J., Baldock, C., Ashworth, J. L., Purslow, P., Shuttleworth, C. A. and Kielty, C. M. (1999). Fibrillin-rich microfibrils of the extracellular matrix: ultrastructure and assembly. *Micron* (in press).

Trask, T. M., Ritty, T. M., Broekelmann, T., Tisdale, C. and Mecham, R. P. (1999). N-terminal domains of fibrillin 1 and fibrillin 2 direct the formation of homodimers: a possible first step in microfibril assembly. *Biochem. J.* **340**, 693-701.

Wilson, R., Allen, A. J., Oliver, J., Brookman, J. L., High., S. and Bulleid, N. J. (1995). The translocation, folding, assembly and redox-dependent degradation of secretory and membrane proteins in semi-permeabilised mammalian cells. *Biochem J.* **307**, 679-687.

Yuan, X., Downing, A. K., Knott, V. and Handford, P. A. (1997). Solution structure of the transforming growth factor beta-binding protein-like module, a domain associated with matrix fibrils. *EMBO J*. **16**, 6659-6666.

Zhang, H., Hu, W. and Ramirez, F. (1994). Structure and expression of fibrillin-2, a novel microfibrillar component preferentially located in elastic matrices. *J. Cell Biol*. **129**, 1165-1176.